ORIGINAL RESEARCH

Assessment of SPO2FRAG software for estimating collapse capacity of steel plate shear walls

Pooya Arezoomand Langarudi[1], Mohammadreza Adibramezani[1,*], Ata Hojatkashani[1] , Saeed Farokhizadeh[1]

Abstract:

Evaluating the seismic vulnerability and collapse capacity of structural systems typically requires performing Incremental Dynamic Analysis (IDA) and developing fragility curves—complex and time-consuming processes. To simplify the derivation of fragility curves across various performance levels, the SPO2FRAG software was introduced in prior research. However, its accuracy in predicting the collapse capacity of systems with varying heights has not been thoroughly validated against detailed seismic analyses. This study examines the efficiency and accuracy of SPO2FRAG for steel plate shear wall systems (SPSWs) with 4, 8, 12, and 16 stories, all designed to comply with relevant codes. The numerical models were validated against a well-documented experimental specimen. Fragility curves at the collapse performance level were developed using two approaches: (1) IDA with 22 pairs of far-field earthquake records and (2) the SPO2FRAG software. The results indicate that for 4- and 8-story buildings, SPO2FRAG provides conservative estimates of collapse capacity compared to the more precise IDA results. However, its reliability diminishes as building height increases, resulting in significant overestimations for the 16-story structure. While SPO2FRAG offers a rapid and cost-effective solution for assessing low- to mid-rise SPSWs, more accurate methods, such as IDA, are recommended for evaluating taller structures. This study highlights the limitations of SPO2FRAG in analyzing high-rise SPSWs and emphasizes the importance of employing detailed analysis methods for critical infrastructure. Future research should focus on enhancing the predictive capabilities of simplified tools like SPO2FRAG for high-rise structures.

Keywords:

Steel Plate Shear Wall (SPSW), Pushover Analysis, Fragility Curve, Incremental Dynamic Analysis (IDA), Performance-based Assessment

*Corresponding author Email: mr_adib@azad.ac.ir

1 Department of Civil Engineering, South Tehran Branch, Islamic Azad University, Tehran, Iran

1. Introduction

Assessing seismic vulnerability and collapse capacity of buildings are fundamental challenges in earthquake engineering. As outlined in the FEMA P695 guidelines [1], the median collapse capacity is a crucial metric for evaluating structural performance. It signifies the seismic intensity at which over 50% of earthquake records lead to structural collapse. This parameter is traditionally calculated using Incremental Dynamic Analysis (IDA) [2], a method renowned for its computational complexity and significant resource requirements.

Historically, engineers have used approximate methods, such as nonlinear static procedures, to estimate the seismic capacity of structures. The iterative nature of load increments in both pushover and IDA methods has motivated researchers to explore relationships between these approaches. Such efforts aim to approximate IDA results while circumventing the time-intensive and computationally demanding analyses it entails.

One notable simplified approach is SPO2IDA [3,4], which uses empirical equations to simulate IDA results based on pushover analysis outcomes. These empirical equations relate the IDA curve to a structure's period and the parameters of its pushover curve. They are derived from an extensive set of IDA results for Single Degree of Freedom (SDOF) oscillators with varying periods and force-displacement characteristics [5,6]. This approach has been incorporated into FEMA P-58 [7,8] for seismic evaluations in the United States, particularly for masonry structures.

Recently, the SPO2IDA methodology has been implemented in MATLAB, resulting in the development of the SPO2FRAG software [9]. This program approximates fragility curves [10] for various performance levels based on a structure's pushover curve. However, the effectiveness and accuracy of SPO2FRAG's results remain subject to further validation.

In prior research on the seismic vulnerability of residential masonry buildings, Yekrangnia [11] utilized SPO2FRAG to generate fragility curves without relying on IDA. Similarly, Shanehsazzadeh et al. [12] applied SPO2FRAG to estimate the collapse capacity of a 12-story reinforced concrete frame, highlighting the time- and resource-intensive nature of IDA. Other researchers have used SPO2FRAG to derive fragility curves for reinforced concrete buildings ranging from 17 to 26 stories [13].

Kaveh et al. [14] applied SPO2FRAG to generate IDA and fragility curves at various damage levels for performance-based optimization. They employed a chaotic algorithm to minimize the total weight of 8- and 20-story composite moment-resisting frames. In another study, SPO2FRAG was applied exclusively for the bilinearization of pushover curves [15].

Although SPO2FRAG has been employed for various concrete, masonry, and composite structures, limited research has examined its accuracy for steel structures with varying numbers of stories. Notably, some studies have used this software to extract analysis results without thoroughly evaluating its efficiency and accuracy in both tall and short structures. This study is the first to analyze steel plate shear walls (SPSWs) of varying heights (4, 8, 12, and 16 stories) using SPO2FRAG and to compare the results with those obtained from precise IDA analyses.

The primary research questions guiding this study are as follows:

- Can the SPO2FRAG software reliably estimate the collapse capacity of steel plate shear walls?
- To what extent do the results from SPO2FRAG align with those from precise IDA analyses?
- Does the accuracy of the SPO2FRAG method vary with an increasing number of stories?

The subsequent sections of this paper address the following topics:

(1) A review of the SPO2FRAG software; (2) Modeling and validation of an experimental steel plate shear wall in OpenSees [16]; (3) A detailed explanation of the SPSW design process based on AISC 341-22 [17]; (4)

Design of the models under study in compliance with relevant codes; (5) Conducting pushover analysis and extracting the capacity curve; (6) Generating fragility curves using the approximate SPO2FRAG method; (7) Performing IDA and generating fragility curves with 22 pairs of far-field earthquake records; (8) Comparing fragility curve results obtained from both methods; and (9) Summary of findings and conclusion.

2. Review of the SPO2FRAG software

The core concept of SPO2FRAG lies in its ability to efficiently predict IDA results for a given SDOF system without requiring extensive additional analyses. This capability is achieved through the SPO2IDA algorithm, which simulates nonlinear dynamic responses. By processing a multi-linear backbone curve derived from a structure's pushover analysis, SPO2IDA estimates the 16th, 50th, and 84th percentiles of the IDA curves. While these estimates are approximate, they significantly reduce the computational effort and time typically associated with traditional IDA procedures. Consequently, SPO2FRAG was developed using this methodology to generate fragility curves for building structures, particularly for concrete structures.

SPO2FRAG features a user-friendly graphical interface that enables users to visualize the results generated by its various modules at each stage. It comprises a set of independent yet complementary modules, including an input interface, an automatic multi-linearization module, a dynamic properties toolbox, the SPO2IDA module, tools for defining limit states and thresholds, options for incorporating additional uncertainty sources, a fragility curve module, and an output post-processing module. Figure 1 illustrates the software's initial graphical interface.

SPO2FRAG does not perform structural analysis; instead, it assumes that the necessary nonlinear static and optional modal analyses have already been completed externally. Each project begins with data input, where the software reads force-displacement results from the pushover analysis, typically imported as a text file or spreadsheet.

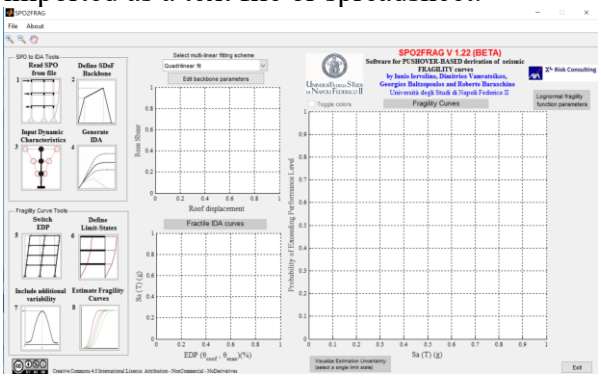

Fig. 1. Initial graphical interface of SPO2FRAG

The workflow within SPO2FRAG comprises the following steps:

Step 1: Data input

The process begins with importing a text file containing two primary columns (Figure 2): the first column represents base shear, and the second corresponds to roof displacement, both derived from the structure's pushover analysis. Upon import, the software immediately generates and displays the pushover curve. Although only roof displacements are required for this step, it is advisable to include displacements at all floors as additional columns in the input file to enhance the comprehensiveness of the analysis. The pushover curve then undergoes preliminary validity and consistency checks.

Subsequently, the roof displacement and base shear data are forwarded to the automatic linear fitting module for further processing.

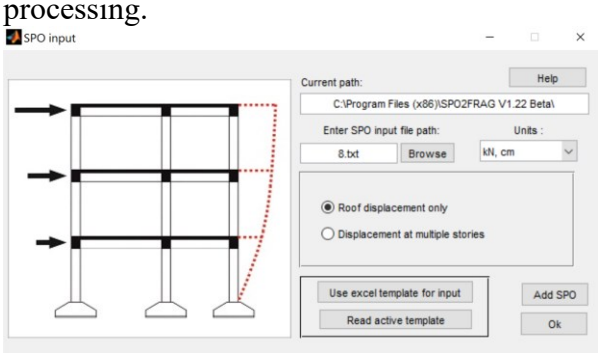

Fig. 2. Inputting the pushover curve

Step 2: Multi-linear fitting

In the subsequent step, the multi-linear fitting module facilitates the definition of the equivalent single-degree-of-freedom (SDOF) backbone curve (Figure 3). A typical pushover curve can generally be segmented into distinct regions: an initial elastic segment leading to yield, a post-yield region characterized by positive stiffness (hardening) up to the peak, a descending branch (softening), and, in certain cases, a residual strength region.

This module offers several fitting options:

1. Four-linear fit
2. Bilinear fit
3. Elastic-perfectly plastic fit
4. Manual user input

All backbone curves generated automatically by the module can be adjusted by the user as required.

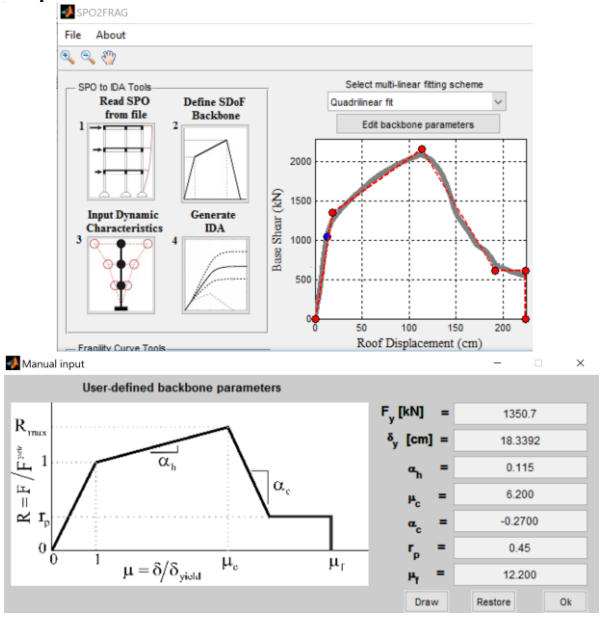

Fig. 3. Defining the backbone curve

Step 3: Defining dynamic properties

After establishing the backbone curve, the next step involves inputting the structure's dynamic properties and geometric configuration (Figure 4). The required inputs include floor and roof masses, the number of stories, story heights, the first and second mode periods, and the mass participation factor. If floor displacements are provided, SPO2FRAG can internally estimate the modal participation factors, mass participation, and the first mode period.

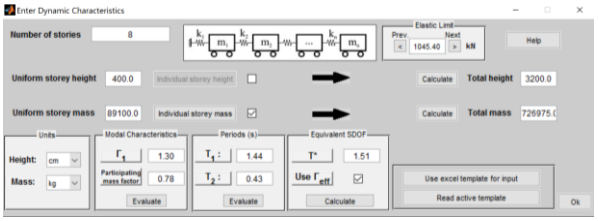

Fig. 4. Defining the dynamic properties and geometric configuration of the structure

Step 4: Running SPO2IDA

Once all required inputs are provided and the multi-linear fitting of the pushover curve is completed, the SPO2IDA algorithm can be executed. This algorithm predicts the 16th, 50th, and 84th percentiles of the IDA curve. The outputs are automatically transformed into a spectral acceleration versus drift format based on the structure's dynamic properties (Figure 5). If displacements at all floor levels are available, the IDA curves are, by default, converted to the maximum interstory drift ratio (IDR). Otherwise, the engineering demand parameter (EDP) defaults to roof drift. However, users can opt to approximate the post-yield lateral deformation profile and convert the results to IDR as needed.

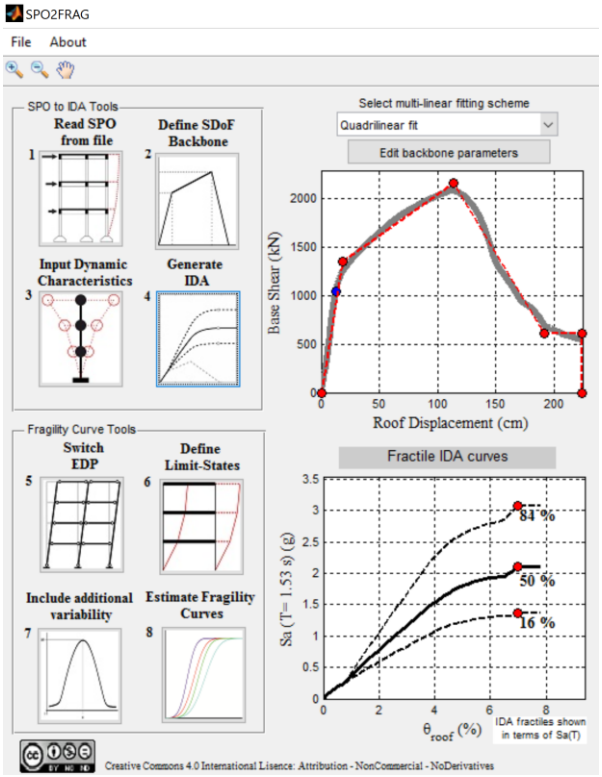

Fig. 5. Extracting IDA curves using SPO2FRAG

Step 5: Defining threshold values for performance limits

At this stage, users define threshold values for various performance limits based on drift values for each performance state (Figure 6). By default, SPO2FRAG includes four predefined limit states:

1. Fully Operational: The structure remains fully functional with no interruptions.
2. Immediate Occupancy: Minor damage may occur, but the structure remains safe for occupancy.
3. Life Safety: Significant damage occurs, but the risk to human life is minimized.
4. Collapse Prevention: Severe damage is present, but complete structural collapse is avoided.

Users can also define additional limit states through the graphical user interface. In all cases, thresholds must be specified in terms of the engineering demand parameter (EDP), which determines when each limit state is exceeded. The EDP represents a structural response measure, such as displacement or acceleration, used to evaluate compliance with performance thresholds.

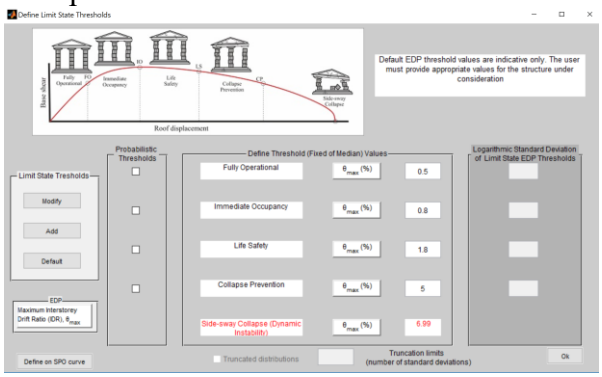

Fig. 6. Defining thresholds for various performance limits

Step 6: Additional settings and fragility Curve generation

Optional settings and parameters can be adjusted to enhance the accuracy of the results, as shown in Figure 7. Upon completing these steps, the fragility function parameters for each limit state are estimated based on the structure's approximate IDA curves. The software then generates fragility curves corresponding to the user-defined performance levels, as illustrated in Figure 8.

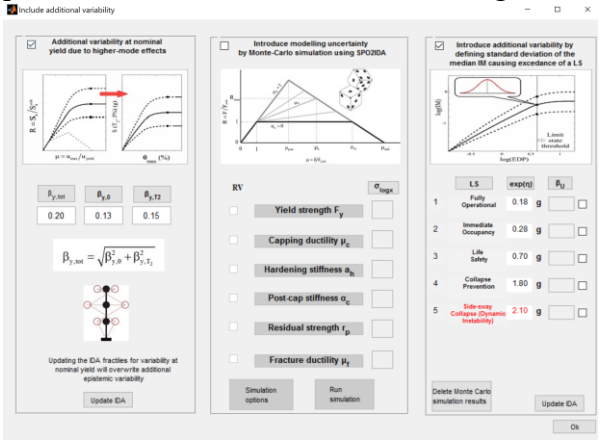

Fig. 7. Defining additional optional variables and parameters

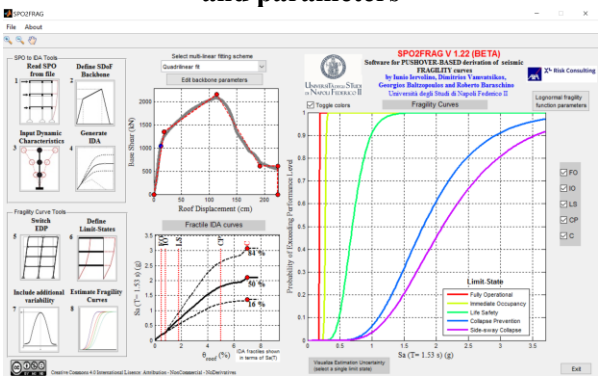

Fig. 8. Generating fragility and IDA curves using SPO2FRAG

3. Modeling and validation of steel plate shear walls

To compare the fragility curves and median collapse capacities derived from the two methods, it is essential to develop an appropriate nonlinear model of the SPSW system for conducting IDA under seismic records. Ensuring the model's accuracy requires accounting for stiffness degradation and strength, making validation against reliable experimental data a critical step [18]. In this study, the validation process was conducted using OpenSees, based on the DS-PSW specimen presented by Sabouri and Sajadi [19].

The boundary elements were modeled with the DispBeamColumn element, a displacement-based distributed plasticity element, incorporating fiber sections. These fiber sections were defined using the uniaxial

Steel02 material, which implements the bilinear Menegotto-Pinto stress-strain model.
In accordance with the recommendations of AISC 341-22, the steel plates were modeled as ten equally spaced strips with pinned ends, utilizing truss elements.
Several hysteresis models have been developed to describe the cyclic response characteristics of steel plate shear walls. Among these, the model proposed by Jalali and Benazadeh [20] stands out for its comprehensive approach to capturing the complex behavior of steel plate shear walls under seismic loading. This model integrates material yield behavior, plate buckling, cyclic and in-cycle degradation, and other critical factors. In this study, the behavioral model proposed by Jalali and Benazadeh has been adopted.
The experimental results were compared with the numerical modeling outputs, demonstrating a high level of agreement, with an average error of less than 5% across key performance metrics. For clarity, the configuration under study and the force-drift comparison between the numerical and experimental models are presented in Figures 9 and 10.

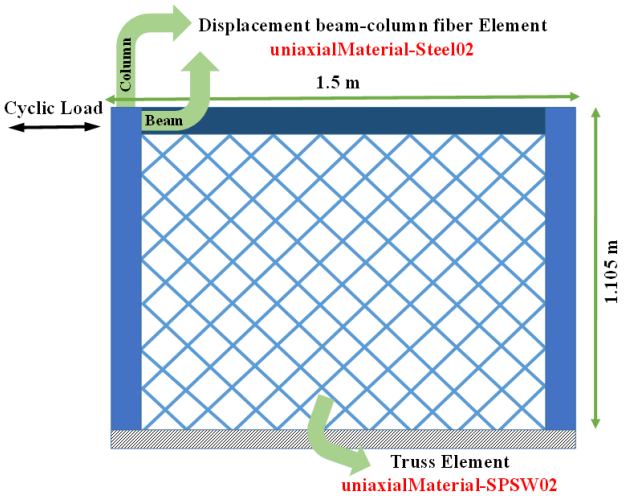

Fig. 9. Configuration of the numerical model in OpenSees

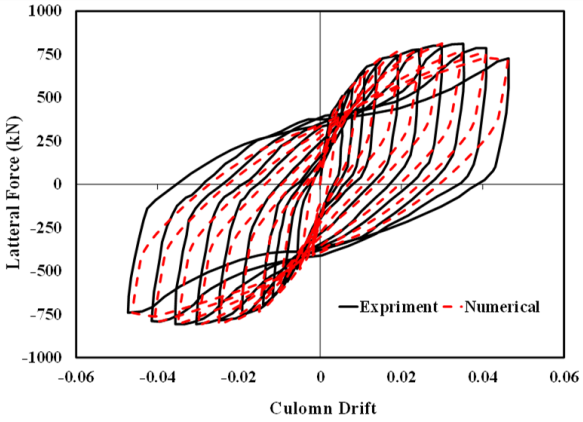

Fig. 10. Comparison of the force-drift curves between the experimental specimen and the numerical model

4. Step-by-step design of steel plate shear walls based on AISC 341-22

The design of the SPSW system was performed per the AISC 341-22 code [14], which outlines seismic design guidelines, including provisions for strength, stiffness, and detailing to achieve ductile performance under seismic loading. The design process was carried out following these steps:

Step 1: Initial angle assumption and plate thickness calculation

An initial inclination angle of 45 degrees was assumed for the tension field action in the steel plates, aligning with the code's acceptable range of 30 to 55 degrees. This angle offers a balanced compromise, simplifies the modeling process, and serves as a suitable starting point for design.
The plate thickness was then calculated using Eq. (1), accounting for 100% of the shear force acting on each floor. This conservative approach ensures that the design accommodates the full shear demand, ensuring the structure's safety and robustness.

$$t_w = \frac{2.645 V_u}{F_u L_{cf} \sin 2\alpha} \quad (1)$$

Where V_u is the required shear strength, F_y is the plate's yield strength, L_{cf} is the distance between column flanges, and α is the plate's yield angle relative to the vertical axis, measured in degrees.

Step 2: Determining the minimum required moment of inertia

The minimum required moments of inertia for the columns and beams were calculated using Eqs. (2) and (3). These values serve as a basis for selecting appropriate preliminary sections for the boundary elements, ensuring sufficient stiffness to achieve the desired ductile behavior and to prevent premature failure.

Minimum moment of inertia for columns:

$$I_c \geq 0.0031 \frac{t_w h^4}{L} \quad (2)$$

Minimum moment of inertia for beams:

$$I_b \geq 0.0031 \frac{\Delta t_w L^4}{h} \quad (3)$$

Where L is the distance between column centers, h is the distance between beam centers, t_w is the plate thickness, and Δt_w is the thickness difference between the top and bottom plates.

Step 3: Recalculating the angle and verifying stress ratios

Following the selection of preliminary sections for the boundary members, the angle α was recalculated using Eq. (4). The plate thickness and stress ratios were then re-evaluated based on this updated angle to ensure the accuracy of the design and to verify that all structural components can adequately resist the applied loads.

$$\tan^4 \alpha = \frac{1 + \frac{t_w L}{2A_c}}{1 + t_w h \left[\frac{1}{A_b} + \frac{h^3}{360 I_c L} \right]} \quad (4)$$

Where A_c and A_b represent the cross-sectional area of the column and beam, I_c is the moment of inertia of the column, and other parameters have been previously defined.

Step 4: Structural analysis and iteration

A structural analysis was conducted, applying concentrated end moments to the beams and considering the forces resulting from the uniform tensile yielding of the plates on the boundary elements. An iterative process was employed to select appropriate sections for all elements, ensuring that the demand-to-capacity ratio for each member was less than or equal to one and that the structure's drift remained within allowable limits.

The entire design process was conducted using MATLAB for code compliance checks and OpenSees for structural analysis. MATLAB's scripting capabilities were particularly useful for automating the iterative selection and optimization of member sections, ensuring adherence to design codes. OpenSees was chosen for its robustness in performing detailed nonlinear analyses, especially in capturing the inelastic behavior and buckling effects of SPSWs. Compared to other software like SAP2000, which is better suited for linear and simple nonlinear analyses, OpenSees offers superior capabilities for modeling complex inelastic responses. The combination of MATLAB and OpenSees ensured accurate verification of design constraints, iterative calculations, and member section optimization, significantly reducing the complexity and time required for manual calculations while minimizing potential errors. The design results are presented in Section 5.

4. Design of the studied models

Four SPSW frames with 4, 8, 12, and 16 stories were selected for this study. Each building features a story height of 4 meters and a bay width of 6 meters. The plan and elevation details, along with the applied loads for the equivalent static analysis, are presented in Figure 11.

Each building utilizes two steel plate shear walls in both directions to resist lateral loads. The structures are designed with a symmetric square plan measuring 18 × 18 meters. The dead loads applied to the floors and roof are 500 kg/m² and 600 kg/m², respectively, while the live loads are 200 kg/m² for the floors and 150 kg/m² for the roof. The boundary elements consist of American W-sections made from ASTM A992 steel (F_y = 345 MPa), and the steel plates used have a yield strength of 239 MPa. All models fall within seismic design category D (with parameters listed in Table 1) and are assumed to be located on site

class D soil. As specified in the American code, all regulations and limitations for steel plate shear walls were fully observed.
The response modification coefficient (R) was set at 7, the deflection amplification factor (C_d) at 6, and an importance factor (I_e) of 1 was used for all structures. While the gravity framing system was not explicitly modeled, leaning columns were incorporated to account for P-Delta effects, as illustrated in Figure 11[21].

Table 1. Seismic design parameters

S_s	S_1	S_{MS}	S_{M1}	S_{DS}	S_{D1}	T_s
1.5	0.6	1.5	0.9	1.0	0.6	0.6

The fundamental period of the buildings was calculated using the method proposed in ASCE 7-22 [22], as expressed in Eq. (5):

$$T = C_t H^x \quad (5)$$

where H represents the height of the building, and for SPSW systems, C_t= 0.05 and x= 0.75. Table 2 provides the base shear coefficient (C_S) values for each model, along with the necessary parameters for their computation, including the fundamental period (T_1) and the corresponding spectral acceleration ($S_a(T_1,5\%)$).

Table 2. Base shear coefficient values

Number of stories	T_1	S_a (T_1,5%)	C_S
4	0.40	1.00	0.142
8	0.67	0.90	0.128
12	0.91	0.65	0.093
16	1.13	0.53	0.076

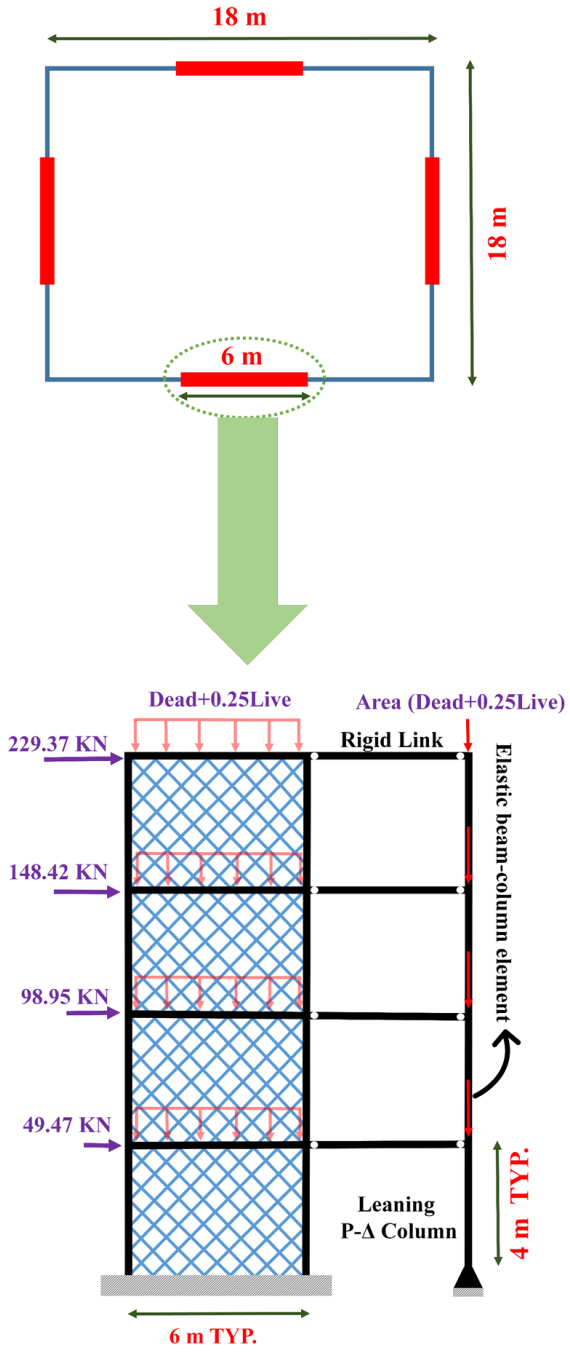

Fig. 11. 4-Story structure model

Table 3 lists the selected sections for the SPSW components, while Figure 12 provides a graphical representation of the stress ratios for each member. The stress ratios are labeled using combinations of letters and numbers, where the letters denote the member type (C: Column, B: Beam, P: Plate) and the numbers correspond to the story level.
Table 4 summarizes the average stress ratios and the inter-story drift ratios for each structure.

Table 3. Selected sections for SPSW components

Number of stories	Floor	4	8	12	16
Columns	16				W14X311
	15				W14X233
	14				W14X233
	13				W14X233
	12			W14X311	*W550
	11			W14X233	W550
	10			W14X233	W550
	9			W14X233	W550
	8		W14X311	W14X233	*W700
	7		W14X176	W14X500	W700
	6		W14X176	W14X500	W700
	5		W14X176	W14X500	W700
	4	W14X311	W14X257	W550	*W750
	3	W14X74	W14X257	W550	W750
	2	W14X132	W14X257	W550	W750
	1	W14X132	W14X257	W550	W750
Beams	16				W14X211
	15				W10X39
	14				W10X39
	13				W10X39
	12			W14X211	W12X136
	11			W10X39	W10X39
	10			W10X39	W10X39
	9			W12X136	W12X136
	8		W14X211	W10X39	W10X39
	7		W10X39	W10X39	W10X39
	6		W12X136	W12X136	W10X39
	5		W10X39	W10X39	W10X39
	4	W14X211	W10X39	W10X39	W12X136
	3	W10X39	W12X136	W10X39	W10X39
	2	W10X39	W10X39	W10X39	W10X39
	1	W10X39	W10X39	W10X39	W10X39
Plates	16				0.10
	15				0.10
	14				0.10
	13				0.10
	12			0.10	0.15
	11			0.10	0.15
	10			0.10	0.15
	9			0.15	0.20
	8		0.10	0.15	0.20
	7		0.10	0.15	0.20
	6		0.15	0.20	0.20
	5		0.15	0.20	0.25
	4	0.10	0.15	0.20	0.25
	3	0.10	0.20	0.20	0.25
	2	0.10	0.20	0.20	0.25

1	0.10	0.20	0.20	0.25

*Sections Wx represent built-up girders with a height of x millimeters that follow the length-to-thickness ratio of W14×370.

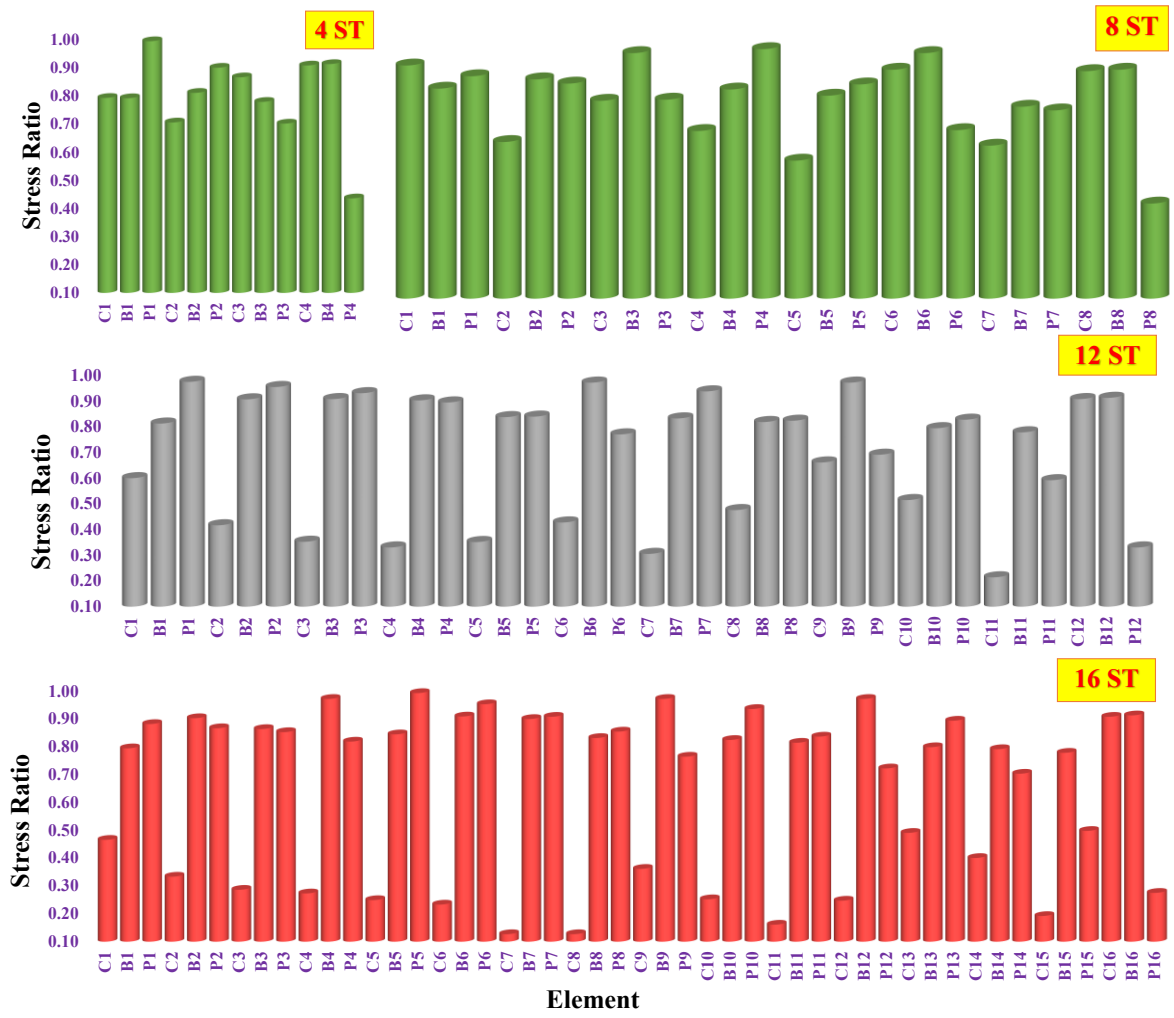

Fig. 12. Stress ratios for each member

Table 4. Average stress ratios and inter-story drift ratios

Number of stories	4	8	12	16
Average stress ratio	0.79	0.80	0.70	0.66
Drift ratio (%)	0.61	0.93	0.97	0.99
Analytical T_1 (s)	0.71	1.19	1.68	2.11

6. Extraction of pushover curves for the models

To estimate the collapse capacity of the structures using the proposed method, pushover analyses were conducted on the SPSW models. The resulting pushover curves were used as input for the SPO2FRAG software to generate fragility curves.

Before applying lateral loads, an initial load comprising gravity loads was applied to each structure, as prescribed by FEMA P695. Subsequently, lateral loads were applied following a triangular distribution pattern, as defined in Eq. (6). The analysis was carried out until the displacement reached 10% of the building height [23].

$$C_{vx} = \frac{W_x h_x^k}{\sum_{i=1}^{ns} W_i h_i^k} \quad (6)$$

where C_{vx} represents the vertical distribution factor at each level, W_x and Wi represent the portion of seismic weight assigned to story x and i, respectively, and h_x and hi are the heights from the base to story x and i. The exponent k is determined using Eq. (7):

$$K = \begin{cases} 1 & T \le 0.5 \\ 2 & T \ge 2.5 \\ 0.5T + 0.75 & 0.5 < T < 2.5 \end{cases} \quad (7)$$

Figure 13 shows the pushover curves for the studied models.

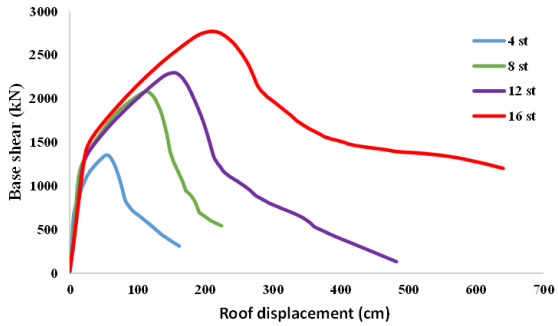

Fig. 13. Pushover curves of the different structures

7. Fragility curve results using SPO2FRAG

Fragility curves are essential tools for assessing the probability of specific failure modes in structures under varying seismic intensities [24,25]. They play a pivotal role in seismic vulnerability assessments. By illustrating the relationship between seismic intensity and the likelihood of damage, fragility curves provide valuable insights into building performance under earthquake conditions.

In this study, the pushover curves of the SPSW frames, introduced in the previous section, were utilized as input to extract fragility curves using SPO2FRAG. The procedure, outlined in Section 2, involves defining the structural model, performing pushover analysis, and using the resulting pushover curves to generate fragility curves. Key steps include selecting appropriate limit states, specifying material properties, and calibrating the model based on experimental data.

Fragility curves at the collapse performance level are depicted in Figures 14–17 using the SPO2FRAG method. In SPO2FRAG, the collapse threshold drift corresponds to the point where the IDA curves generated by the software begin to flatten, indicating the onset of structural instability.

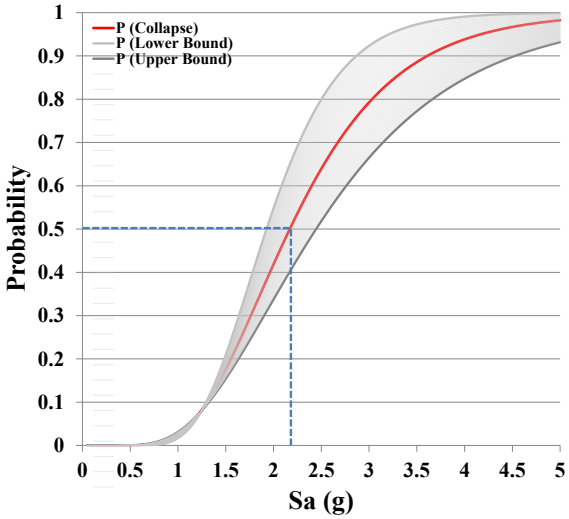

Fig. 14. Fragility curve for 4-story structure using SPO2FRAG

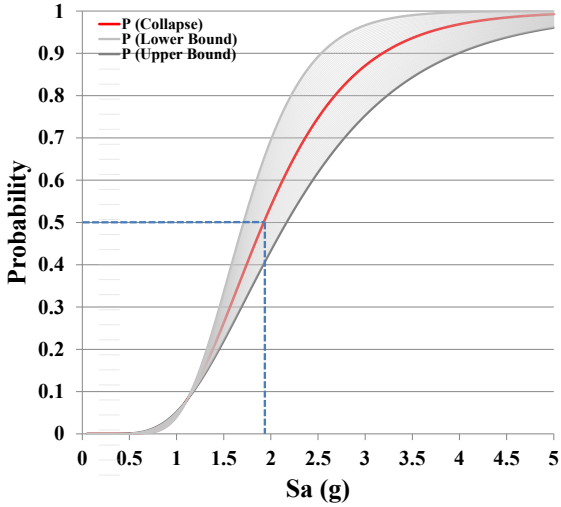

Fig. 15. Fragility curve for 8-story structure using SPO2FRAG

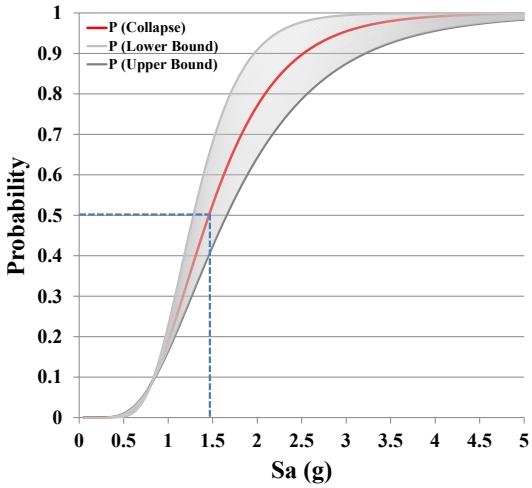

Fig. 16. Fragility curve for 12-story structure using SPO2FRAG

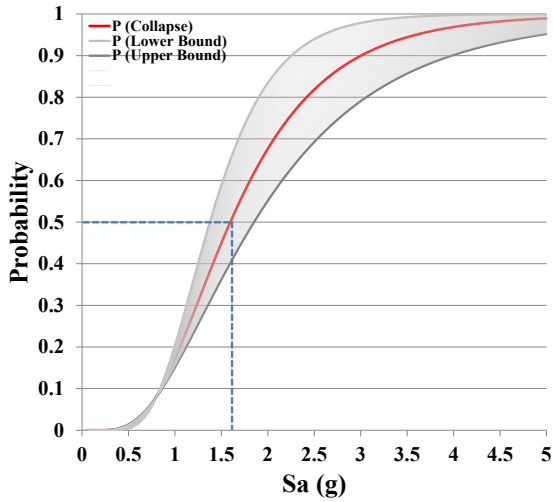

Fig. 17. Fragility curve for 16-story structure using SPO2FRAG

8. Fragility curve results using IDA

The IDA technique involves performing a series of nonlinear dynamic analyses on each seismic record to evaluate the full range of structural responses comprehensively. In this study, the primary objective of these analyses was to estimate the median collapse capacity of the structures ($\hat{S}_{CT}$), enabling quantitative comparison between this precise method and the approximate SPO2FRAG method. $\hat{S}_{CT}$ represents the intensity level at which more than 50% of the seismic records cause structural collapse. This value can be calculated for each model using fragility curves derived from detailed IDA results. For the IDA, 44 far-field seismic records (22 pairs) recommended by FEMA P695 were utilized. Nonlinear dynamic analyses were conducted on each model, with the seismic records scaled linearly until structural collapse was observed. Over 2,500 analyses were performed across the four models. The resulting IDA curves illustrate the relationship between the spectral intensity of ground motion, expressed as the Intensity Measure (IM) on the vertical axis, and the maximum inter-story drift, represented as the Engineering Demand Parameter (EDP) on the horizontal axis. Figure 19 displays the IDA curves for all models, including the 16th, 50th, and 84th percentiles, alongside IDA curves generated using the SPO2FRAG method for direct comparison.

The collapse point is defined as the intensity level where the local slope of the IDA curve decreases to 20% of the elastic slope or where the maximum inter-story drift reaches 10% [26]. These criteria were chosen because they effectively represent the onset of significant inelastic deformation and degradation of structural stiffness, which are critical indicators of potential collapse. Both criteria were applied in this study to define collapse points, which served as thresholds for identifying structural failure and plotting fragility curves at the collapse performance level. Figure 18 illustrates the fragility curves obtained from the precise IDA method at this level.

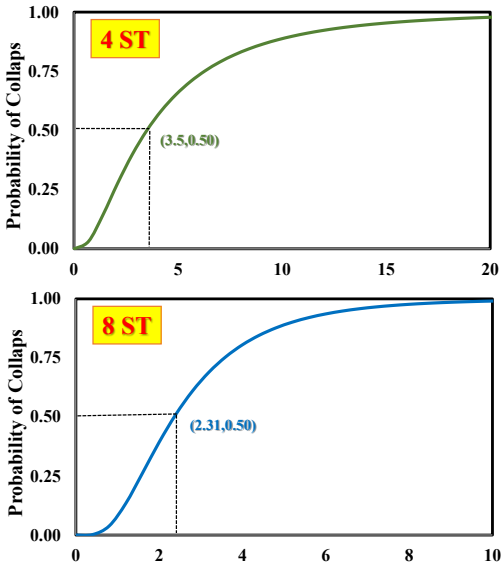

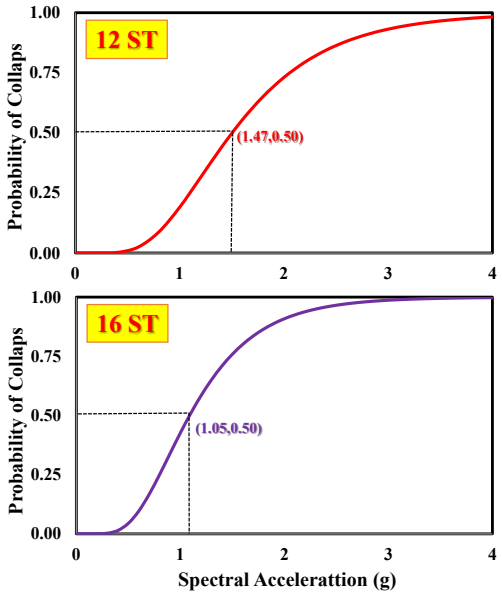

Fig. 18. Fragility curves of different structures at collapse level using the IDA method

9. Comparison of results from the two methods

Figure 19 compares the IDA curves derived from the two methods, focusing on the 16th, 50th, and 84th percentiles. These percentiles represent a range of possible structural responses: the 16th percentile corresponds to a lower-bound (less severe) response, the 50th percentile reflects the median (typical) response, and the 84th percentile signifies an upper-bound (more severe) response.

The graphs reveal that SPO2FRAG underestimates the percentiles for the 4-story structure but overestimates them for taller structures. However, for most structures, except the 16-story building, the 50th percentile results from SPO2FRAG show reasonably good agreement with the IDA results derived from the 22 pairs of seismic records.

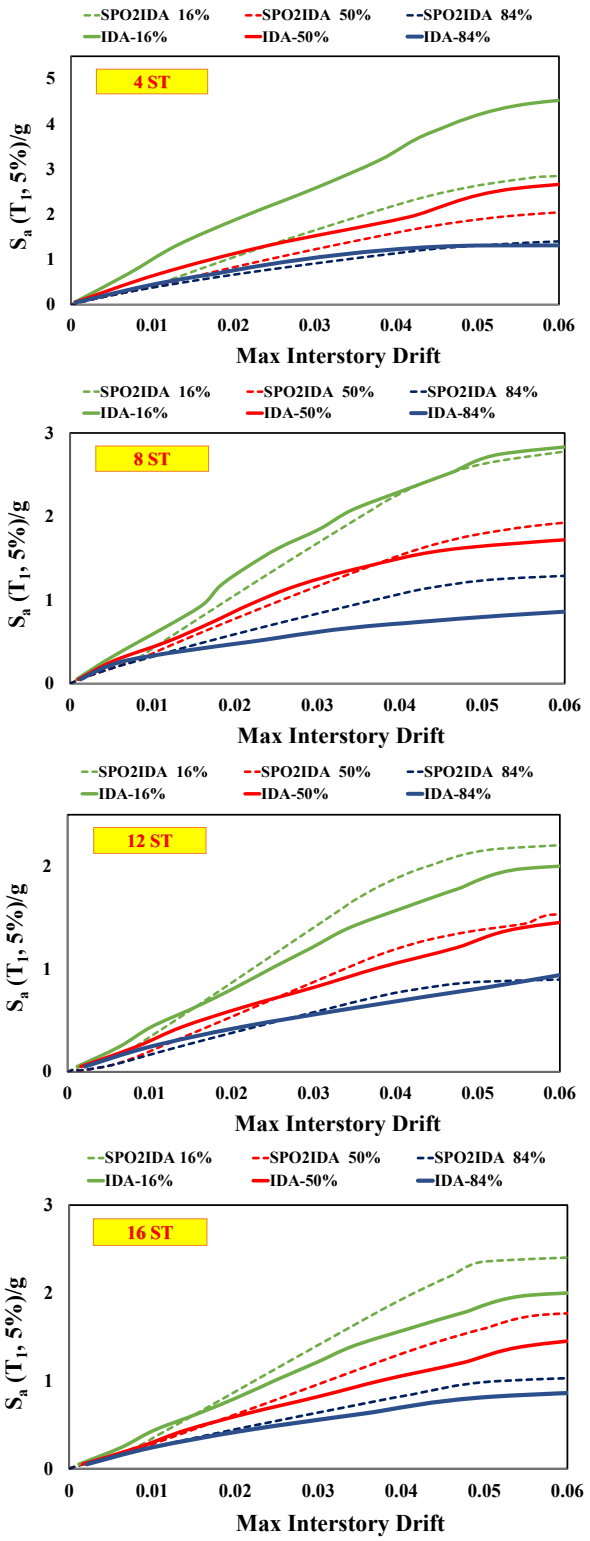

Fig. 19. Comparison of IDA curves from the two methods

The comparison of median collapse capacity values obtained from fragility curves generated using SPO2FRAG and IDA is summarized in Table 5. As discussed in

Sections 7 and 8, the SPO2FRAG method generally provides more conservative estimates for shorter structures, whereas the IDA method yields more precise and reliable results, particularly for taller structures. In summary, SPO2FRAG tends to deliver conservative estimates for shorter buildings, while IDA is preferred for more accurate assessments, especially in the case of taller buildings.

In Table 5, a positive percentage difference indicates that the SPO2FRAG method overestimates the median collapse capacity compared to IDA, whereas a negative percentage difference signifies that SPO2FRAG provides a more conservative (lower) estimate. For the 4- and 8-story structures, SPO2FRAG underestimates the median collapse capacity by 38% and 16.9%, respectively. For the 12-story structure, the overestimation is minimal at only +2%. However, for the 16-story structure, SPO2FRAG overestimates the median collapse capacity by 51.4%. This leads to the conclusion that SPO2FRAG is not recommended for tall structures. When precision is critical, particularly in determining the response modification coefficient in accordance with FEMA P695, the IDA method remains the preferred approach.

The results of this study are contingent upon the specific assumptions and parameters used in the analyses. Any changes to these factors may lead to different outcomes, highlighting the need for further investigation. Future research should focus on improving the accuracy and efficiency of simplified methods, such as the SPO2FRAG software, for estimating fragility curves at various performance levels, particularly for tall buildings, to enable more robust and reliable assessments.

Table 5. Comparison of median collapse capacity values obtained from the two methods

Structure	4	8	12	16
IDA method	3.50	2.31	1.47	1.05
SPO2FRAG	2.17	1.92	1.50	1.59
Difference percentage	-38.0	-16.9	+2.0	+51.4

10. Summary and conclusion

This study evaluated the accuracy and efficiency of the SPO2FRAG software in predicting the collapse capacity of steel plate shear wall (SPSW) structures. A numerical model of an SPSW system was validated against experimental data, followed by the design of 4-, 8-, 12-, and 16-story structures using MATLAB and OpenSees. Fragility curves for these structures were generated using both SPO2FRAG and the precise Incremental Dynamic Analysis (IDA) method, and the results were compared. The key findings of the study are summarized as follows:

1. SPO2FRAG significantly reduces computational effort compared to IDA, making it a viable alternative for preliminary analyses.
2. For structures with up to 12 stories, SPO2FRAG produces acceptable results, often providing conservative estimates when compared to IDA.
3. For 4- and 8-story structures, SPO2FRAG underestimates the median collapse capacity by up to 38% compared to IDA.
4. As the number of stories increases, the accuracy of SPO2FRAG decreases, resulting in less reliable predictions for taller structures.
5. For structures taller than 12 stories, the IDA method is recommended.
6. If sufficient computational resources are available, IDA should be employed for more precise analyses, particularly for tall and critical structures.

11. References

[1]. FEMA P695 (2009), *Quantification of building seismic performance factors*, Washington, DC: Federal Emergency Management Agency.

[2]. Bernuzzi, C., Rodigari, D. and Simoncelli, M. (2020). Incremental dynamic analysis for assessing the seismic performance of moment resisting

steel frames, *Ingegneria Sismica*, 37 (4), 23-44.

[3]. Vamvatsikos, D. and Allin Cornell, C. (2006). Direct estimation of the seismic demand and capacity of oscillators with multi-linear static pushovers through IDA, *Earthquake Engineering & Structural Dynamics*, 35 (9), 1097-1117.

[4]. Ren, Y., Ma, D., Wang, W., Guo, X., Wang, Z., Chen, D., Wu, J., Fei, Z. and Zhao, X. (2024). Application of SPO2IDA in Seismic Performance Evaluation of Ancient Timber Structures, *International Journal of Architectural Heritage*, 18 (8), 1308-1322. https://doi.org/10.1080/15583058.2023.2221215.

[5]. Zou, X., Gong, M., Zuo, Z. and Liu, Q. (2024). An efficient framework for structural seismic collapse capacity assessment based on an equivalent SDOF system, *Engineering Structures*, 300 117213. https://doi.org/10.1016/j.engstruct.2023.117213.

[6]. Suzuki, A. and Iervolino, I. (2021). Seismic Fragility of Code-conforming Italian Buildings Based on SDoF Approximation, *Journal of Earthquake Engineering*, 25 (14), 2873-2907. 10.1080/13632469.2019.1657989.

[7]. FEMA-P-58 (2012), *Seismic performance assessment of buildings*, Washington, D.C., USA: Federal Emergency Management Agency.

[8]. Nafeh, A. M. B. and O'Reilly, G. J. (2024). Simplified pushover-based seismic loss assessment for existing infilled frame structures, *Bulletin of Earthquake Engineering*, 22 (3), 951-995. 10.1007/s10518-023-01792-x.

[9]. Baltzopoulos, G., Baraschino, R., Iervolino, I. and Vamvatsikos, D. (2017). SPO2FRAG: software for seismic fragility assessment based on static pushover, *Bulletin of Earthquake Engineering*, 15 4399-4425. https://doi.org/10.1007/s10518-017-0145-3.

[10]. Nafeh, A. M. B. and O'Reilly, G. J. (2022). Unbiased simplified seismic fragility estimation of non-ductile infilled RC structures, *Soil Dynamics and Earthquake Engineering*, 157 107253. https://doi.org/10.1016/j.soildyn.2022.107253.

[11]. Yekrangnia, M. (2023). Seismic Vulnerability Assessment of Masonry Residential Buildings in the Older Parts of Tehran through Fragility Curves and Basic RVS Scores, *Buildings*, 13 (2), https://doi.org/10.3390/buildings13020302.

[12]. Shanehsazzadeh, H., Tehranizadeh, M. and Haj Najafi, L. (2023). Evaluation of the Collapse Capacity Ratio of the Near Fault to the Far Fault and Its Effect on Collapse Risk in Terms of Pulse Period and Formability, *Bulletin of Earthquake Science and Engineering*, 10 (3), 31-48. https://doi.org/10.48303/bese.2022.557180.1085.

[13]. Ugalde, D., Lopez-Garcia, D. and Parra, P. F. (2020). Fragility-based analysis of the influence of effective stiffness of reinforced concrete members in shear wall buildings, *Bulletin of Earthquake Engineering*, 18 (5), 2061-2082. https://doi.org/10.1007/s10518-020-00786-3.

[14]. Kaveh, A., Mahdipour Moghanni, R. and Javadi, S. M. (2022). Chaotic optimization algorithm for performance-based optimization design of composite moment frames, *Engineering with Computers*, 38 (3), 2729-2741. https://doi.org/10.1007/s00366-020-01244-z.

[15]. Sococol, I., Mihai, P., Petrescu, T.-C., Nedeff, F., Nedeff, V., Agop, M. and Luca, B.-I. (2022). Numerical Study Regarding the Seismic Response of a Moment-Resisting (MR) Reinforced Concrete (RC) Frame Structure with Reduced Cross-Sections of the RC Slabs, *Buildings*, 12 (10), 1525. https://doi.org/10.3390/buildings12101525.

[16]. Mazzoni, S., McKenna, F., Scott, M. H. and Fenves, G. (2004). OpenSees users manual, *PEER, University of California, Berkeley*, 18 56-57.

[17]. ANSI/AISC 341-22 (2022), *Seismic Provisions for Structural Steel Buildings*, Chicago (IL): American Institute for Steel Construction.

[18]. Akbarpour, a., Eftekhari, m. m. and Roudsari, M. T. (2023). Study of Scale Effect on Seismic Performance of Steel Plate Shear Wall under Cyclic Loading, *International Journal of Advanced Structural Engineering*, 4 (13), 1-14. 10.30495/ijase.2023.708020.

[19]. Sabouri-Ghomi, S. and Sajjadi, S. R. A. (2012). Experimental and theoretical studies of steel shear walls with and without stiffeners, *Journal of Constructional Steel Research*, 75 152-159. https://doi.org/10.1016/j.jcsr.2012.03.018.

[20]. Jalali, S. A. and Banazadeh, M. (2016). Development of a new deteriorating hysteresis model for seismic collapse assessment of thin steel plate shear walls, *Thin-Walled Structures*, 106 244-257. https://doi.org/10.1016/j.tws.2016.05.008.

[21]. Arezoomand Langarudi, P., Adibramezani, M., Hojatkashani, A. and Farokhizadeh, S. (2024). Effect of Design Optimality and Overstrength on the Seismic Performance of Steel Plate Shear Walls, *Iranian Journal of Science and Technology, Transactions of Civil Engineering*, https://doi.org/10.1007/s40996-024-01513-7.

[22]. ASCE/SEI 7-22 (2022), *Minimum design loads for buildings and other structures*, Reston: American Society of Civil Engineering.

[23]. Arezoomand Langarudi, P. and Ebrahimnejad, M. (2020). Numerical study of the behavior of bolted shear connectors in composite slabs with steel deck, *Structures*, 26 501-515. https://doi.org/10.1016/j.istruc.2020.04.037.

[24]. BahariPour, S., Nani, M., Hosseini, M., Moghadam, A. s. and Razzaghi, M. M. S. (2023). Performance Evaluation and Comparison of Schools with Masonry System Treated by Braces, FRP Strips and Friction Dampers Using Fragility Curves (Case Study: Khorram Abad), *International Journal of Advanced Structural Engineering*, 3 (13), 0-0. 10.30495/ijase.2023.1992357.1075.

[25]. Zentner, I., Gündel, M. and Bonfils, N. (2017). Fragility analysis methods: Review of existing approaches and application, *Nuclear Engineering and Design*, 323 245-258. https://doi.org/10.1016/j.nucengdes.2016.12.021.

[26]. Vamvatsikos, D. and Cornell, C. A. (2002). Incremental dynamic analysis, *Earthquake Engineering & Structural Dynamics*, 31 (3), 491-514. https://doi.org/10.1002/eqe.141.